Abdominal Radiology

Published online: 1 November 2018

Abdom Radiol (2019) 44:1070–1082
https://doi.org/10.1007/s00261-018-1816-5

MRI of testicular malignancies

Athina C. Tsili,[1] Nikolaos Sofikitis,[2] Efrosyni Stiliara,[1] and Maria I. Argyropoulou[1]

[1]Department of Clinical Radiology, Medical School, University of Ioannina, University Campus, 45110 Ioannina, Greece
[2]Department of Urology, Medical School, University of Ioannina, University Campus, 45110 Ioannina, Greece

Abstract

Although testicular carcinoma represents approximately only 1% of solid neoplasms in men, it is the most common malignancy between young men. The two main histologic categories are testicular germ cell tumors (TGCTs), including seminomas and nonseminomas, accounting for 90–95% of testicular neoplasms and sex cord-stromal tumors. Scrotal MRI, including a multiparametric protocol, has been proposed as a valuable supplemental imaging technique in the investigation of testicular pathology. Recently, the Scrotal and Penile Imaging Working Group appointed by the board of the European Society of Urogenital Radiology has produced recommendations on when to perform scrotal MRI. Regarding intratesticular masses, MRI of the scrotum may be used for their characterization, when US findings are indeterminate and for local staging of TGCTs, when organ-sparing surgery is planned. Differentiation between seminomas and nonseminomas is possible based on MRI features, when clinically needed. Scrotal MRI may also help in differentiating between TGCTs and nongerm cell tumors. Functional information based on diffusion-weighted imaging and dynamic contrast-enhanced MRI data improve testicular mass lesion characterization. Preliminary observations on diffusion tensor imaging, magnetization transfer imaging, and proton MR spectroscopy bring about new data in the understanding of testicular microstructure and pathophysiology.

Key words: Magnetic resonance imaging—Testis—Testicular neoplasms—Testicular germ cell tumors

Testicular cancer represents 1% of male neoplasms and 5% of urological tumors. However, it is the commonest malignancy among young men, aged 15–35 years, accounting for 10-14% of cancer incidence in that age group [1, 2]. The American Cancer Society estimates that during 2018, 9.310 men will develop testicular cancer and 400 men will die of this disease [3]. Clinically, testicular carcinoma usually presents as a painless, scrotal swelling or a palpable mass, as an incidental US finding or revealed during the investigation of scrotal trauma, while acute pain may be the presenting symptom in 20% of cases [1, 2].

The predominant histology is testicular germ cell tumor (TGCT), accounting for approximately 90–95% of testicular carcinomas [4]. TGCTs are evenly split into two broad categories: seminomas and nonseminomatous germ cell tumors (NSGCTs) [4]. Approximately 4% of all testicular tumors in the adult population arise from the cells forming the sex cords and the interstitial stroma, with Leydig cell tumor (LCT) representing the most common testicular sex cord-stromal tumor [4]. The majority of these tumors are benign. Pathologic features that are suspicious for malignancy include large tumor size, infiltrative margins, lymphovascular invasion, necrosis, nuclear atypia, and frequent or atypical mitoses [4].

Currently, US, including conventional gray scale and color Doppler US, represents the initial modality for the confirmation of the presence of a testicular mass and for the assessment of the contralateral testis [2, 3, 5, 6]. US is a sensitive and accurate technique for the evaluation of testicular diseases and should be performed even in the presence of clinically evident testicular tumor [2, 3].

MRI has emerged as a worthwhile second-line imaging diagnostic tool for the investigation of testicular pathology, especially recommended in cases of discrepancies between US findings and clinical history so that radical orchiectomy can be avoided in cases of benign lesions [6–17].The advantages of the technique include simultaneous imaging of both testes, paratesticular spaces, and spermatic cords, high contrast and spatial resolution, satisfactory anatomic and functional information, absence of radiation exposure, and less dependence on operator technique compared to US [6–17]. Recently, the Scrotal and Penile Imaging Working

Correspondence to: Athina C. Tsili; *email:* a_tsili@yahoo.gr, atsili@cc.uoi.gr

Group (SPIWG) of the European Society of Urogenital Radiology (ESUR) has produced recommendations on imaging acquisition protocols and clinical indications for MRI of the scrotum [18]. Regarding testicular malignancies, scrotal MRI may be used for lesion characterization and local staging of TGCTs and for characterization of the histologic nature of TGCTs in selected cases [18]. The role of MRI in differentiating between TGCTs and nongerm cell neoplasms is still evolving [18].

Recent advances in scrotal MRI using a multiparametric protocol which combines morphological and functional data significantly improved the diagnostic performance of the technique in the characterization of intratesticular masses [19–34]. Diffusion-weighted imaging (DWI) and dynamic contrast-enhanced (DCE) MRI should be routinely included in the MRI protocol of the scrotum [19–28]. Moreover, promising preliminary data on diffusion tensor imaging (DTI), magnetization transfer imaging (MTI), and proton MR spectroscopy (1H-MRS) of the testis have been reported [29–34].

In this pictorial essay, clinical indications for MRI of the scrotum in cases of testicular carcinomas are reviewed. Conventional MRI findings of testicular malignancies are presented, and the role of functional MRI in characterizing testicular tumors is discussed.

Testicular malignancies: clinical indications for scrotal MRI

Intratesticular mass lesion characterization

Although the presence of intratesticular mass is highly suspicious for malignancy, a possible diagnosis of various benign intratesticular mass lesions, including dilated rete testis, epidermoid cyst, intratesticular lipoma, testicular fibrosis, isolated orchitis, segmental testicular infarction, hematoma, Leydig's cell hyperplasia, and adrenal rests based on imaging findings has been shown to improve patient management and reduce healthcare costs. In these cases, a conservative approach can be adopted, including follow-up, biopsy, tumor enucleation, and organ-sparing surgery [9, 10, 12, 15, 17].

Scrotal MRI has been proved an accurate and cost-effective diagnostic modality for the characterization of intratesticular masses, recommended as a problem-solving tool in cases of solid testicular lesions with indeterminate findings, based on clinical and US examination [18]. MRI features, including tumor location, morphologic information, and tissue characterization, may help by showing the presence of fat, blood products, fibrosis, fluid, granulomatous tissue, and solid contrast-enhancing tissue [9, 10, 12, 15, 17, 35, 36].

Conventional MRI findings of TGCTs closely correlate with gross and microscopic characteristics [35, 37]. TGCTs often have similar T1 signal, when compared to normal testicular parenchyma, appear hypointense or heterogeneous, with variable signal intensity on T2-weighted imaging (T2WI), and enhance inhomogeneously after gadolinium administration (Figs. 1, 2, 3, 4, 5) [35]. Secondary findings used to confirm the diagnosis of testicular malignancy include the following: presence of areas of hemorrhage (detected with T1 hyperintensity, Fig. 3B) and/or necrosis (detected as hyperintense T2 areas, with the absence of contrast enhancement, Fig. 3D) and extension of the tumor to the testicular tunicae, paratesticular space, and/or the spermatic cord (Figs. 1A, 2B, 4A, B) [35].

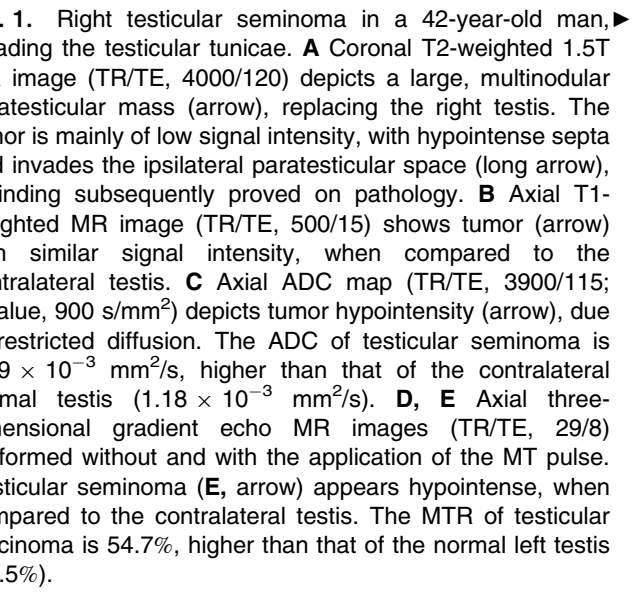

Fig. 1. Right testicular seminoma in a 42-year-old man, invading the testicular tunicae. **A** Coronal T2-weighted 1.5T MR image (TR/TE, 4000/120) depicts a large, multinodular intratesticular mass (arrow), replacing the right testis. The tumor is mainly of low signal intensity, with hypointense septa and invades the ipsilateral paratesticular space (long arrow), a finding subsequently proved on pathology. **B** Axial T1-weighted MR image (TR/TE, 500/15) shows tumor (arrow) with similar signal intensity, when compared to the contralateral testis. **C** Axial ADC map (TR/TE, 3900/115; *b* value, 900 s/mm^2) depicts tumor hypointensity (arrow), due to restricted diffusion. The ADC of testicular seminoma is 0.59×10^{-3} mm^2/s, higher than that of the contralateral normal testis (1.18×10^{-3} mm^2/s). **D, E** Axial three-dimensional gradient echo MR images (TR/TE, 29/8) performed without and with the application of the MT pulse. Testicular seminoma (**E,** arrow) appears hypointense, when compared to the contralateral testis. The MTR of testicular carcinoma is 54.7%, higher than that of the normal left testis (46.5%).

Local staging of TGCTs

Radical orchiectomy with division of the spermatic cord at the internal inguinal ring is the treatment of choice in cases of testicular malignancies [2]. Although organ-sparing surgery is not advocated in the presence of nontumoral contralateral testis, it can be performed in special circumstances, including the presence of synchronous bilateral testicular malignancies, metachronous contralateral tumors, or tumor in a solitary testis with normal preoperative testosterone levels [2]. Accurate preoperative knowledge of the local extent of carcinomas is important in patients who are candidates for testis-sparing surgery.

MRI may be used for local staging of TGCTs [18]. The technique provides important information regarding the local extent of testicular malignancies, including tumor dimensions, possible invasion of the rete testis, testicular tunicae, epididymis and/or paratesticular space, and spermatic cord (Figs. 1A, 2B, 4A, B) [9, 17, 35, 37, 38]. The accuracy of MRI in local staging of TGCTs is reported up to 93% [35]. The presence of tumor pseudocapsule, reported to aid in lesion enucleation when organ-sparing surgery is planned, is another useful information provided by MRI [17, 35].

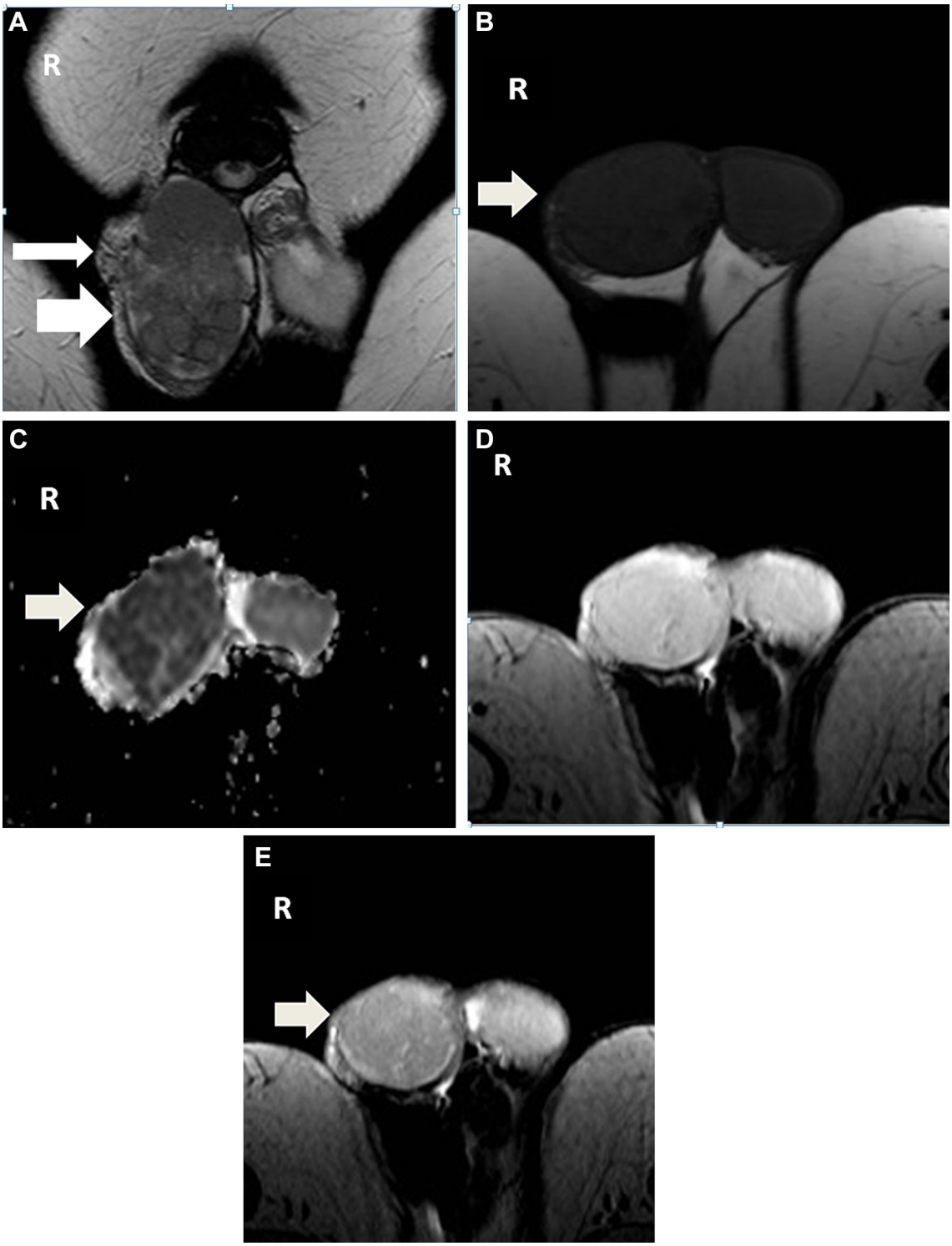
A
R
B
R
C
R
D
R
E
R

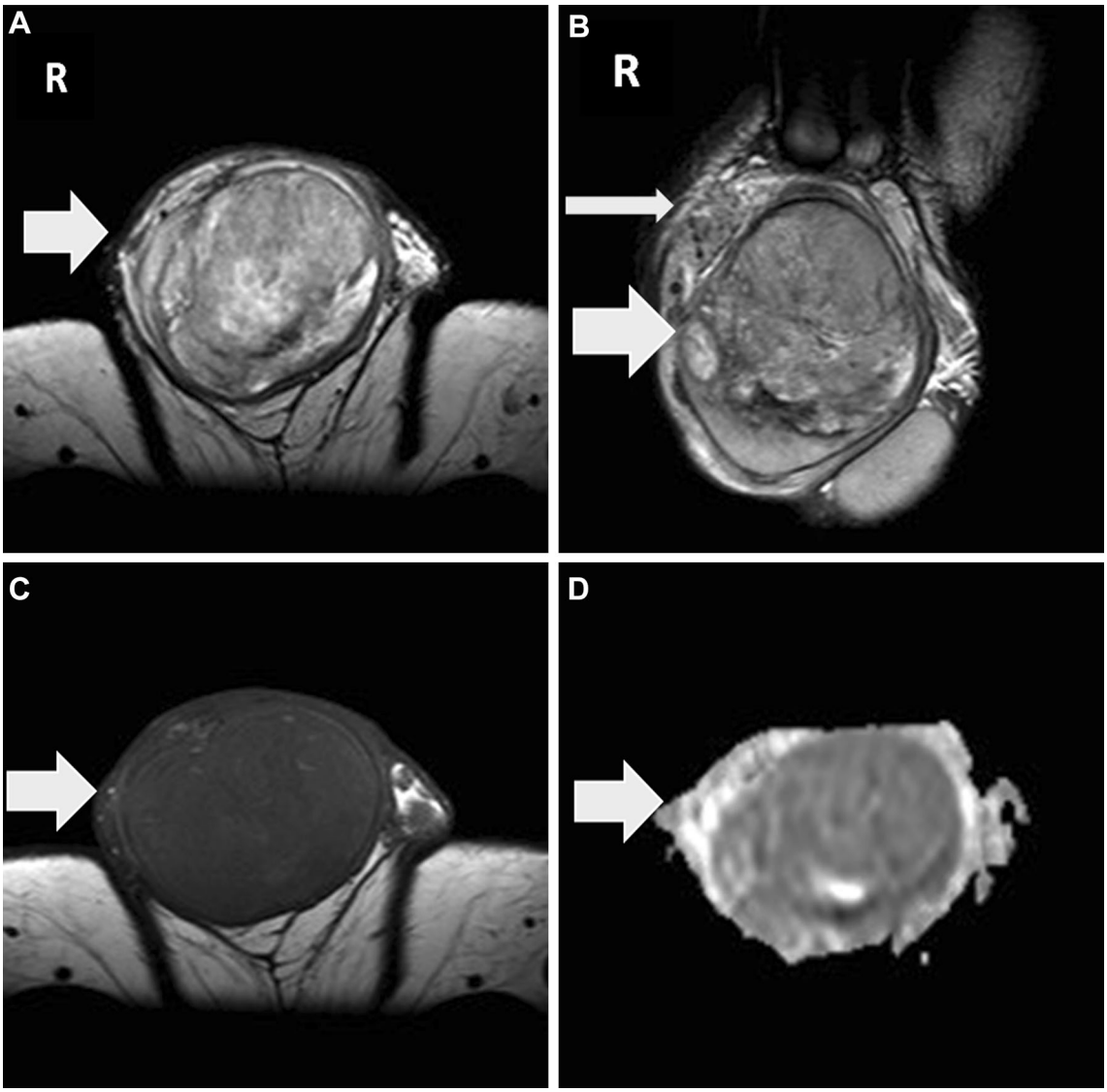

Fig. 2. NSGCT (embryonal carcinoma) of the right testis in a 22-year-old man. **A, B** 1.5T T2-weighted MR images (TR/TE, 4000/120) in axial and coronal planes depict a large, heterogenous mass (arrow), replacing the right testis. The tumor is seen invading the ipsilateral paratesticular space (long arrow in B), as proved on histopathology. **C** Axial T1-weighted MR image (TR/TE, 500/15) shows tumor (arrow) mainly isointense, when compared to the normal contralateral testis (not shown in this image). **D** Axial ADC map (TR/TE, 3900/115; *b* value, 900 s/mm^2) depicts tumor hypointensity (arrow), due to restricted diffusion. The ADC of testicular malignancy is 0.83 $\times$ 10^{-6} mm^2/s.

Histologic characterization of TGCTs

Radical orchiectomy should be performed without any delay if a testicular malignancy is found, unless clinical indications require immediate chemotherapy [2]. Specifically, in patients with disseminated disease and life-threatening metastases, chemotherapy should be initiated and orchiectomy may be delayed, until clinical stabilization occurs or in combination with resection of residual lesions [2]. In these cases, the preoperative differentiation between seminomas and NSGCTs is important.

MRI features have been found closely to correlate with the histologic characteristics of TGCTs, providing a preoperative classification of the histologic type of testicular malignancies up to 91% of cases [37]. Typical testicular seminomas appear as multilonodular neoplasms, mainly homogeneous, with low T2 signal. Band-like structures, hypointense on T2WI, are often detected within seminomas, enhancing more than the remaining tumor after gadolinium administration (Figs. 1A, 4A, B, 5A, B, F) [7, 9, 37–41]. These structures correspond to fibrovascular septa on pathology. NSGCTs on the other hand, are more often markedly heterogeneous, both on unenhanced and contrast-enhanced MR images, and this is correlated with the presence of areas of hemorrhage and/or necrosis on pathology (Fig. 2, 3). Another char-

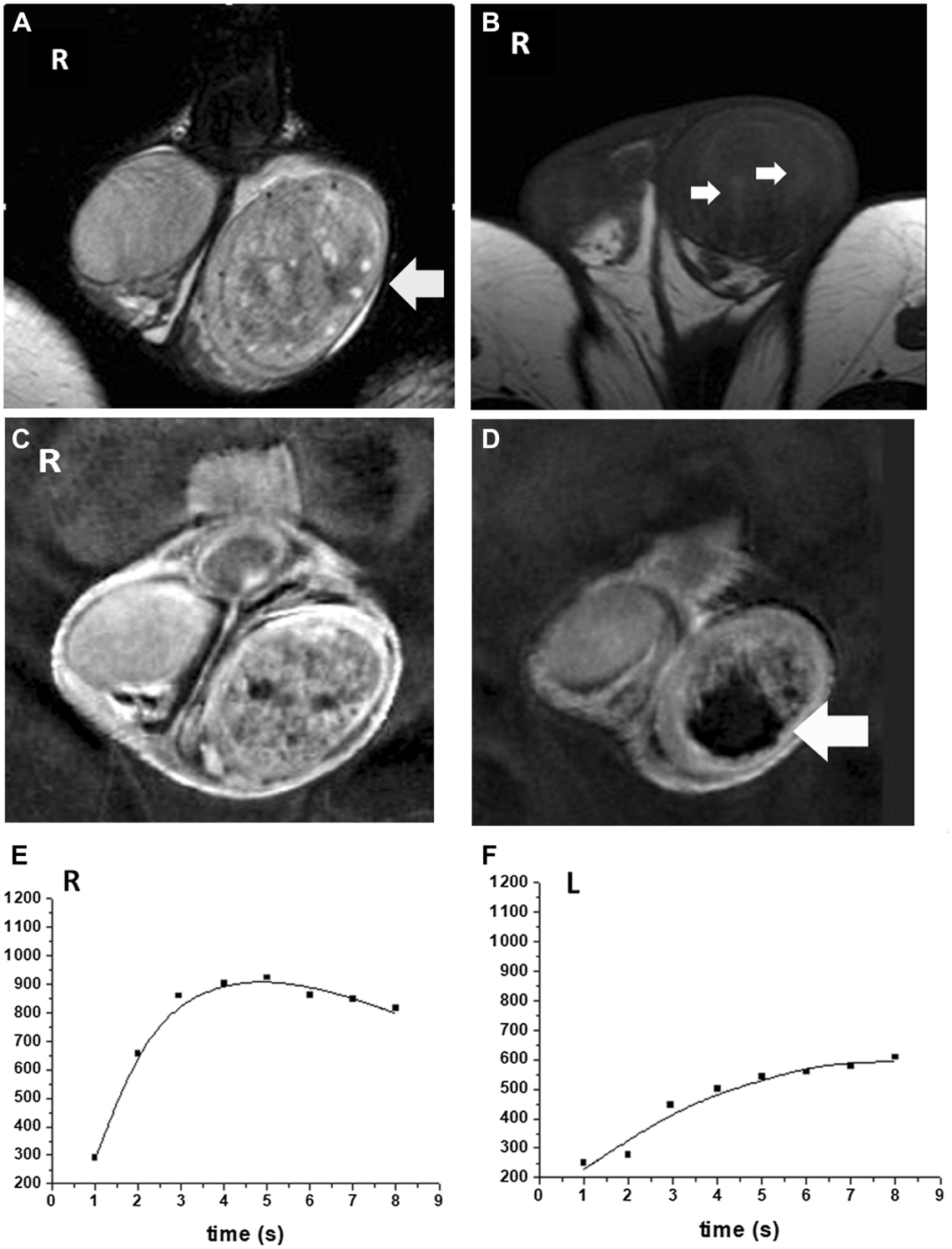

Fig. 3. NSGCT (teratoma, embryonal carcinoma and yolk sac tumor) of the left testis in a 20-year-old man. **A** Coronal T2-weighted 1.5T MR image (TR/TE, 4000/120) depicts a large, heterogenous left intratesticular tumor (arrow). Normal contralateral testis. **B** Axial T1-weighted MR image (TR/TE, 500/15) demonstrates slightly hyperintense areas (small arrows) within the neoplasm, corresponding to areas of hemorrhage on histopathology. **C, D** Coronal subtracted DCE MR images (TR/TE, 4.5/2.2) depict heterogenous tumor enhancement. Large nonenhancing area (arrow in **D**) within the mass due to necrosis, as subsequently proved on histopathology. **E, F** TSI curves of the neoplasm and the contralateral normal testis. The tumor depicts brisk, early enhancement, followed by gradual deenhancement (type III, **E**). The normal right testis presents a linear increase of contrast enhancement throughout the examination (type I, **F**).

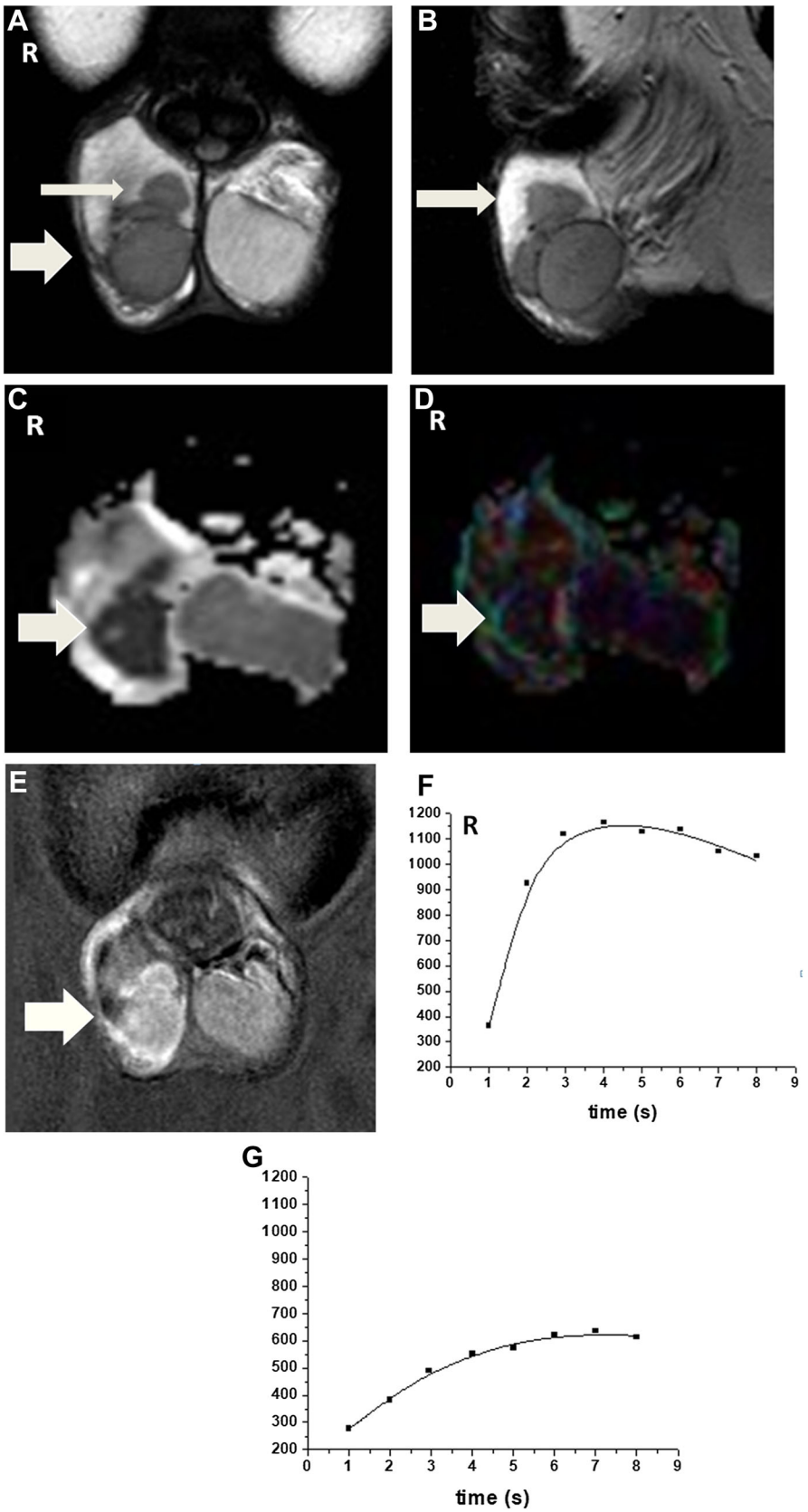
A
R
B
C
R
D
R
E
F
R
1200
1100
1000
900
800
700
600
500
400
300
200
0 1 2 3 4 5 6 7 8 9
time (s)
G
1200
1100
1000
900
800
700
600
500
400
300
200
0 1 2 3 4 5 6 7 8 9
time (s)

◀**Fig. 4.** Right testicular seminoma in a 34-year-old man. **A, B** 1.5T T2-weighted MR images (TR/TE, 4000/120) in coronal and sagittal planes demonstrate a large, mainly homogeneous right intratesticular tumor (arrow), of low signal intensity, when compared to the normal contralateral testis. Fibrovascular septa are detected within the neoplasm as hypointense bands. The tumor is seen invading the paratesticular space (long arrow), as proved on histology. **C, D** Coronal ADC and color-coded FA maps (TR/TE, 3756/131; *b* value, 700 s/mm^2) show restricted tumor diffusion (arrow, **C**). The ADC of testicular seminoma is 0.64×10^{-3} mm^2/s, lower than that of the contralateral testis (1.30×10^{-3} mm^2/s). Testicular malignancy has anisotropic diffusion (arrow, **D**) when compared to the normal left testis, with high FA values (0.25 vs 0.11). **E** Coronal subtracted DCE MR image (TR/TE, 4.5/2.2) depicts heterogenous tumor enhancement (arrow). **F** TSI curve of the tumor (type III). **G** TSI curve of the contralateral normal testis (type I).

acteristic for nonseminomatous tumors is the presence of pseudocapsule, detected as a hypointense halo surrounding the neoplasm [7, 9, 37, 40, 41].

Differentiation between TGCTs and nongerm cell neoplasms

During the last years, the widespread use of scrotal US has resulted in an increase in the detection of impalpable, small incidentally found testicular masses, which up to 80% of cases are benign, with LCTs representing the most common histology [42]. Organ-sparing surgery in every small sonographically detected, nonpalpable intratesticular mass lesion is highly recommended in order to obtain a histologic diagnosis [2].

MRI may help in the characterization of LCTs, although conventional features are often nonspecific [15, 18, 26, 43]. LCTs have been reported as isointense on T1-weighted imaging (T1WI) and hypointense on T2WI compared with the normal testis, markedly and homogeneously enhancing after intravenous contrast medium administration [15]. These neoplasms may also demonstrate a peripheral high T2 signal and a hyperintense central scar on T2WI [15, 44].

Manganaro et al. described the MRI features that can be used to differentiate LCTs from seminomas in cases of small, impalpable, incidentally detected testicular tumors [26]. The presence of a well-defined mass, markedly hypointense on T2WI, with homogeneous contrast enhancement has been reported as more suggestive of the diagnosis of LCTs (Fig. 6) [26]. On the contrary, seminomas were more often detected with ill-defined margins, weak hypointense T2 signal, and weak T1 hyperintensity [26].

Functional MRI techniques

Diffusion-weighted imaging

DWI is a functional MRI technique based on the assessment of increased or restricted microscopic diffusion movements of water molecules in tissues. Lesion detection and characterization are mainly influenced by tissue cellularity, and increased cellularity is reflected by restricted diffusion and reduced apparent diffusion coefficient (ADC) [44, 45].

Regarding testicular malignancies, improvements in the differentiation of testicular lesions and the preoperative characterization of the histologic type of TGCTs have been reported with the addition of DWI [19–23]. The accuracy of conventional MRI data alone, DWI, and DWI combined with conventional imaging in the characterization of testicular lesions has been reported 91, 87, and 100%, respectively [19]. TGCTs typically have low ADC compared to normal testicular parenchyma and benign testicular lesions (Figs. 1C, 2C, 5C) [19, 20]. A cutoff ADC of less than 0.99×10^{-3} mm^2/s had a sensitivity of 93.3%, a specificity of 90%, a positive predictive values of 87.5%, and a negative predictive value of 94.7% in the characterization of testicular lesions [20]. Moreover, ADC can be used as an additional tool in the preoperative characterization of the histologic subtype of TGCTs. The ADC of seminomas has been reported significantly lower compared to that of NSGCTs, with an optimal ADC cutoff of 0.68×10^{-3} mm^2/s (Figs. 1C, 2C, 5C) [22]. Histologic characteristics of testicular seminomas, including the presence of large neoplastic cells, with large nuclei surrounded by fibrous trabeculae and accompanied by lymphocytic infiltrates, plasma cells, eosinophils, and granulomatous reaction probably explain the significant restriction in the movement of water molecules caused by these tumors [4].

Currently, existing data to support the role of DWI in differentiating TGCTs from nongerm cell neoplasms are limited, including series with few and small-sized LCTs [27]. ADC was reported similar for small-sized, impalpable testicular seminomas, and LCTs (Fig. 6C) [27]. Although the majority of LCTs represent benign neoplasms, pathologic features, such as the presence of medium to large polygonal cells with abundant cytoplasm and prominent nucleoli, a rich vascular network, and sometimes a prominent and hyalinized stroma, could result in impended diffusion [4].

Dynamic contrast-enhanced MRI

Dynamic contrast-enhanced (DCE) MRI has been reported useful in the differentiation of testicular lesions [24–28]. Typically, TGCTs show heterogeneous contrast enhancement, with an early, brisk enhancement, followed by gradual washout of the contrast medium with time, characterized as a type III time-signal intensity (TSI) curve (Figs. 3C–E, 4E, F) [25]. The patterns of enhancement for benign testicular lesions vary from absence of enhancement (type 0 curve) to homogeneous or heterogeneous contrast enhancement, presenting an avid, upstroke enhancement, followed by either a plateau, or a

slight further increase during the dynamic study (type II curve) [25, 28]. Normal testes enhance homogeneously and moderately with gradual linear increase of enhancement with time (type I curve), a finding probably related to the intact blood-testis barrier (Fig. 3F) [24, 25]. The relative percentages of peak height and mean slope of TGCTs have been reported significantly higher than those of benign testicular lesions, with the relative percentages of maximum time to peak proving the most important discriminating factor in lesion characterization [24, 25]. No differences in DCE MRI patterns between seminomas and nonseminomas have been reported [22].

DCE MRI may help to differentiate LCTs from seminomas in cases of small, impalpable, incidentally detected testicular tumors [26–28]. LCTs usually present with rapid and marked wash-in, followed by a prolonged washout (Fig. 6E, F), while seminomas display weak, progressive wash-in and absent washout [26]. Recently, Manganaro et al. showed that semiquantitative and pharmacokinetic DCE MRI data are useful in the characterization of small, solid testicular tumors [27]. LCTs usually have higher percentage of peak enhancement, wash-in-rate (WIR), volume transfer constant, rate constant, initial area under the curve, and shorter time to peak when compared to seminomas. WIR was reported with the best diagnostic performance, detected typically earlier and more marked in LCTs [27].

Diffusion tensor imaging

Molecular diffusion is basically a three-dimensional process; therefore, molecular mobility in tissues may be anisotropic. Diffusion tensor imaging (DTI) plots the relative degree of diffusion in multiple directions, providing direct and in vivo information on the organization in space of oriented tissues, such as brain and spine white matter, muscle, myocardium, kidneys, prostate, breast, and uterus [46, 47]. DTI measures both ADC and fractional anisotropy (FA), providing significant improvement in the characterization of tissue microstructure and pathophysiology [46, 47].

Normal testis has a well-defined structure, with seminiferous tubules, septa, and vessels radiating toward the mediastinum [29]. Therefore, testis diffusion is expected anisotropic. However, based on the results of a preliminary study in a 1.5T magnet, with the use of two *b* values (0 and 700 s/mm^2), normal testicular parenchyma had an isotropic diffusion pattern [29]. In the same report, DTI proved useful in the characterization of various testicular lesions [29]. TGCTs often have low ADC and high FA (Fig. 4C, D), due to the fact that diffusion in malignancies is more restricted and more anisotropic, when compared to normal tissues and benign entities. Higher cellularity, increased amount of cell membranes, and intracellular viscosity and significantly decreased extracellular space are probably responsible for the increase in directionality of water diffusion in testicular malignancies.

Fig. 5. Left testicular seminoma in a 28-year-old man. **A, B** ▶ 1.5T T2-weighted MR images (TR/TE, 4000/120) in coronal and sagittal planes demonstrate a multinodular tumor, replacing the left testis. The mass is mainly of low signal, with hypointense septa (small arrow). **C** Axial ADC map (TR/TE, 3900/115; *b* value, 900 s/mm^2) shows tumor (arrow) with low signal intensity, due to water movement restriction. The ADC of testicular malignancy is 0.54×10^{-3} mm^2/s, lower than that of the contralateral normal testis (1.08×10^{-3} mm^2/s). **D, E** Axial three-dimensional gradient echo MR images (TR/TE, 29/8) performed without and with the application of the MT pulse. The MTR of testicular carcinoma (arrow) is 56.7%, higher than that of the normal right testis (46.8%). **F** Coronal subtracted DCE MR image (TR/TE, 4.5/2.2) depicts inhomogeneous tumor enhancement, with fibrovascular septa (small arrow) enhancing more than the remaining tumor. **G** Proton MR spectrum (TR/TE, 2000/25) of testicular seminoma depicts high levels of choline (Cho) and lipids (L).

Magnetization transfer imaging

Magnetization transfer imaging (MTI) is based on the interactions between free water protons and restricted protons, those bound to proteins and macromolecules. With the use of an off-resonance radiofrequency pulse, the magnetization of restricted protons becomes saturated and then transferred to more free protons, causing a reduction in the tissue signal [48]. Tissues with macromolecules transfer magnetization more efficiently and are detected with low signal on MT images. The MTI phenomenon is quantified by MT ratio (MTR) [48].

In normal adult testis, a mean MTR of 46.2% has been reported [30]. The presence of endoplasmic reticulum and collagen are the principal contributing factors to the MT effects of normal testicular parenchyma [30]. The efficacy of MTI in the characterization of testicular malignancies has recently been reported [30]. TGCTs usually have a high MTR (Figs. 1D, E, 5D, E), when compared to normal testis and benign testicular lesions, rendering MTI an adjunct tool in testicular mass lesion characterization [30]. The presence of fibrovascular septa in seminomas and tumor heterogeneity, with the presence of areas of hemorrhage in nonseminomas, might explain the increase in MTR in testicular malignancies [30].

MR spectroscopy

Magnetic resonance spectroscopy (MRS) is an advanced imaging technique used as an adjunct to MRI to provide additional, noninvasive information about the biochemical environment of imaged tissues [49, 50]. Protons

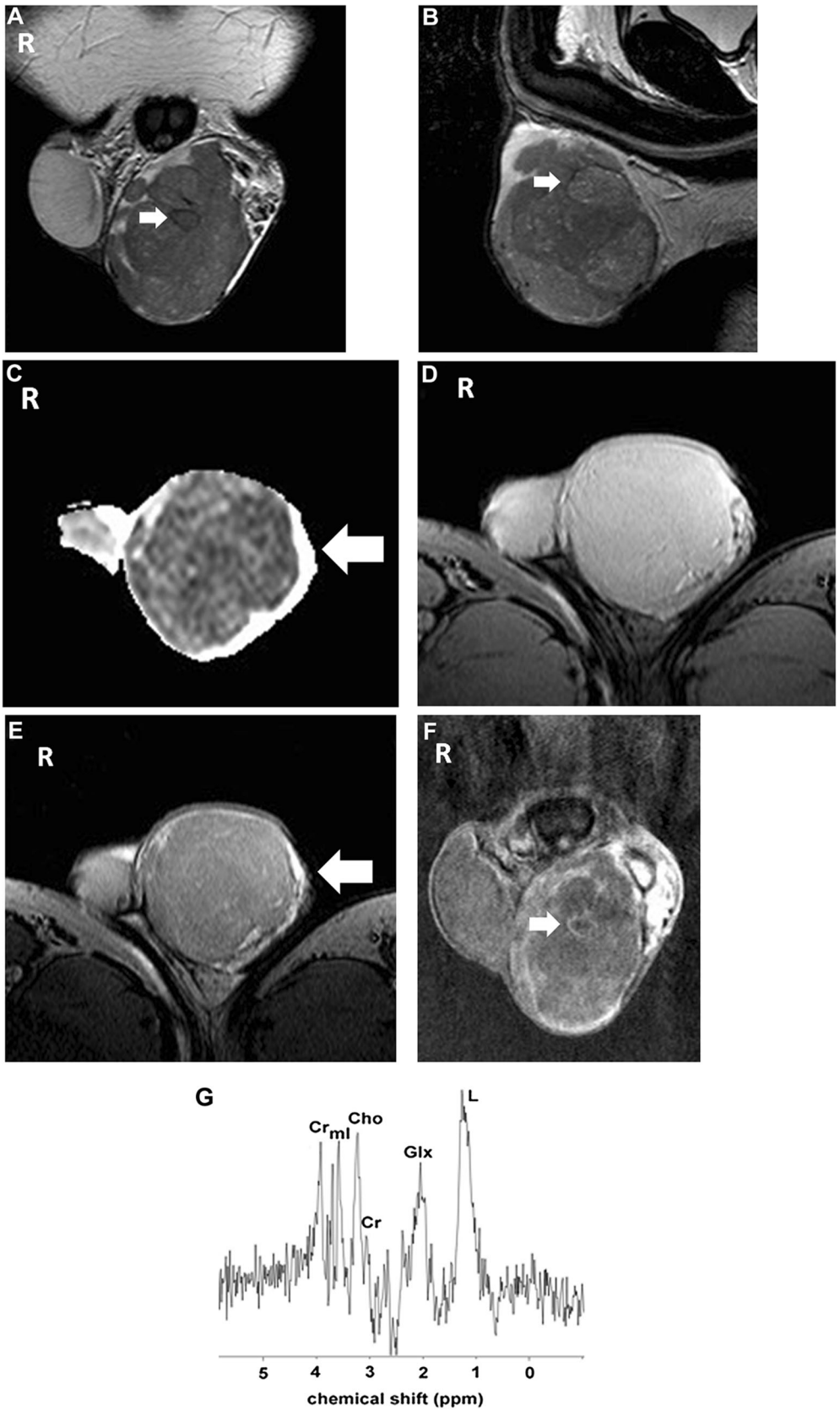
A
R
B
C
R
D
R
E
R
F
R
G
Cr
mI
Cho
Cr
Glx
L
5
4
3
2
1
0
chemical shift (ppm)

(1H) have been traditionally used for MRS, due to their high natural abundance in organic structures and high nuclear magnetic sensitivity [49, 50].

A limited number of published reports have assessed the efficacy of 1H-MRS in the evaluation of testicular metabolic integrity in humans [31–34]. The most prominent metabolic peaks in normal adult testis are those of choline (Cho), creatine, myo-inositol, and lipids (Fig. 7) [33]. Elevated choline peak is considered the most important MRS hallmark for the diagnosis of cancer (Fig. 5G) [49, 50]. Regarding testicular malignancies, data on the utility of MRS are scarce [34]. A sensitivity and specificity of 80% have been reported for MRS using differences between Cho levels and ratio of choline/lipids in differentiating normal testis from various testicular diseases [34]. However, Cho peak in testicular malignancies was found markedly decreased [34]. Whether this observation is associated with impairment in spermatogenesis or concomitant difficulties in detecting Cho peaks in tumors within the adult testis, which normally has high levels of Cho, remains to be elucidated.

Conclusion

Although US continues to represent the imaging modality of choice for the initial investigation of testicular masses, MRI, including a multiparametric protocol, has emerged as an efficient, complimentary diagnostic tool for testicular imaging. Regarding testicular malignancies, scrotal MRI may be used for the characterization of intratesticular masses with indeterminate findings, based on clinical and US examination helping to narrow the differential diagnosis and to determine more precise treatment strategies. The technique performs well in the preoperative evaluation of the local extent of testicular germ cell tumors in cases which may be candidates for organ-sparing surgery. MRI features closely correlate with the histopathologic characteristics of TGCTs and may be used for the classification of the histologic type of testicular tumors in selected cases. MRI may also help in differentiating TGCTs from nongerm cell neoplasms, especially in cases of small, impalpable incidentally discovered testicular tumors. Functional MRI, including diffusion-weighted imaging, dynamic contrast-enhanced MRI, diffusion tensor imaging, magnetization transfer imaging, and 1H MR spectroscopy have added important information in testicular mass lesion characterization.

Fig. 6. Leydig cell tumor of the right testis in a 32-year-old man incidentally discovered on US examination. **A** Sagittal T2-weighted 1.5T MR image (TR/TE, 4000/120) depicts a small right intratesticular mass (arrow). The lesion appears sharply delineated, mainly homogeneous and hypointense, with a maximal diameter of 7 mm. **B** Axial T1-weighted MR image (TR/TE, 500/15) demonstrates lesion slightly hyperintense (arrow) **C, D** Coronal ADC and color-coded FA maps (TR/TE, 3756/131; *b* value, 700 s/mm^2) show lesion hypointense (**C**) and hyperintense (**D**), respectively (arrow), findings indicative of restricted diffusion and increased anisotropy. Measurements of ADC and FA values were difficult to taken, due to the small size of the mass. **E, F** Coronal subtracted DCE MR image (TR/TE, 4.5/2.2) and TSI curve of the lesion show mass (arrow) homogeneously enhancing, with early, strong contrast enhancement, followed by rapid washout of the contrast medium (type III, **F**). ▶

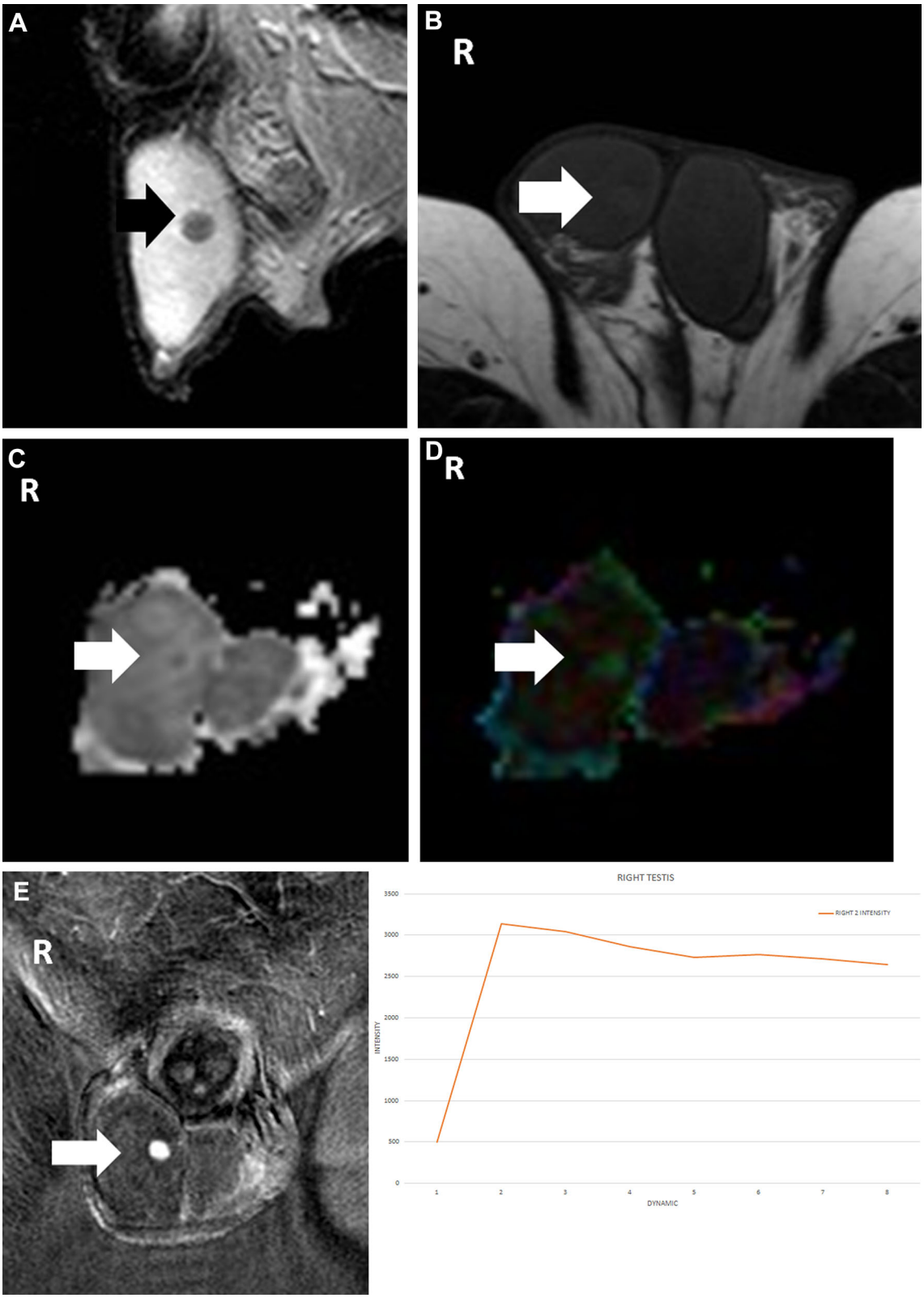
A
B
R
C
R
D
R
E
R
RIGHT TESTIS
RIGHT 2 INTENSITY
INTENSITY
DYNAMIC
3500
3000
2500
2000
1500
1000
500
0
1
2
3
4
5
6
7
8

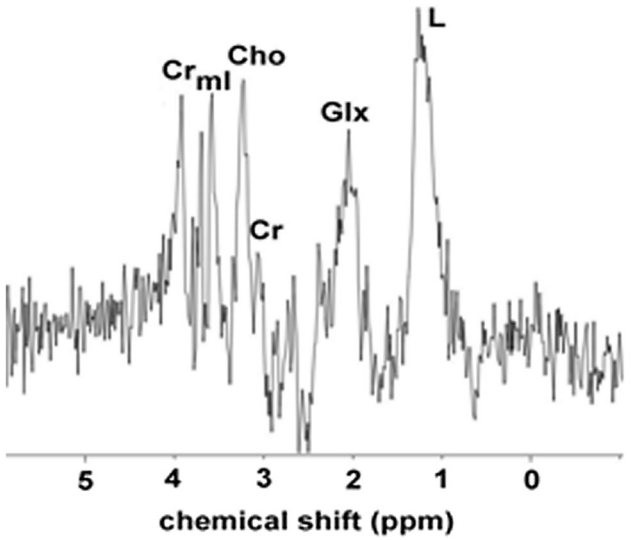

Fig. 7. Normal proton MR spectrum (1.5T) of the right testis in a 25-year-old man shows as prominent metabolite peaks the following: creatine (Cr), myo-inositol (mI), Cho, glutamine and glutamate (Glx) and L and macromolecules.

Compliance with ethical standards

Funding This project received no funding.

Conflict of interest The authors declare that they have no conflict of interest.

Informed consent Not applicable.

References

1. Yacoub JH, Oto A, Allen BC, et al. (2016) ACR appropriateness criteria staging of testicular malignancy. J Am Coll Radiol 13:1203–1209. https://doi.org/10.1016/j.jacr.2016.06.026
2. Albers P, Albrecht W, Algaba F, et al. (2015) Guidelines on testicular cancer: 2015 update. Eur Urol 68:1054–1068. https://doi.org/10.1016/j.eururo.2015.07.044
3. American Cancer Society. Cancer facts & figures 2018. https://doi.org/https://www.cancer.org/content/dam/cancer-org/research/cancer-facts-and-statistics/annual-cancer-facts-and-figures/2018/cancer-facts-and-figures-2018.pdf.
4. Moch H, Cubilla AL, Humphrey PA, Reuter VE, Ulbright TM (2016) The 2016 WHO classification of tumours of the urinary system and male genital organs-part A: renal, penile, and testicular tumours. Eur Urol 70:93–105. https://doi.org/10.1016/j.eururo.2016.02.029
5. Dogra VS, Gottlieb RH, Oka M, Rubens DJ (2003) Sonography of the scrotum. Radiology 227:18–36. https://doi.org/10.1148/radiol.2271001744
6. Mathur M, Mills I, Spektor M (2017) Magnetic resonance imaging of the scrotum: pictorial review with ultrasound correlation. Abdom Radiol 42:1929–1955. https://doi.org/10.1007/s00261-017-1127-2
7. Cramer BM, Schlegel EA, Thueroff JW (1991) MR imaging in the differential diagnosis of scrotal and testicular disease. Radiographics 11:9–21. https://doi.org/10.1148/radiographics.11.1.1996400
8. Oyen R, Verellen S, Drochmans A (1993) Value of MRI in the diagnosis and staging of testicular tumors. J Belge Radiol 76:84–89
9. Kim W, Rosen MA, Langer JE, et al. (2007) US MR imaging correlation in pathologic conditions of the scrotum. Radiographics 27:1239–1253. https://doi.org/10.1148/rg.275065172
10. Woodward PJ, Sohaey R, O'Donoghue MJ, Green DE (2002) From the archives of the AFIP: tumors and tumorlike lesions of the testis: radiologic-pathologic correlation. Radiographics 22:189–216. https://doi.org/10.1148/radiographics.22.1.g02ja14189
11. Serra AD, Hricak H, Coakley FV, et al. (1998) Inconclusive clinical and ultrasound evaluation of the scrotum: impact of magnetic resonance imaging on patient management and cost. Urology 51:1018–1021. https://doi.org/10.1016/S0090-4295(98)00097-1
12. Mohrs OK, Thoms H, Egner T, et al. (2012) MRI of patients with suspected scrotal or testicular lesions: diagnostic value in daily practice. AJR Am J Roentgenol 199:609–615. https://doi.org/10.2214/AJR.11.7349
13. Muglia V, Tucci S Jr, Elias J Jr, et al. (2002) Magnetic resonance imaging of scrotal diseases: when it makes the difference. Urology 59:419–423. https://doi.org/10.1016/S0090-4295(01)01579-5
14. Tsili AC, Giannakis D, Sylakos A, et al. (2014) MR imaging of scrotum. Magn Reson Imaging Clin N Am 22:217–238. https://doi.org/10.1016/j.mric.2014.01.007
15. Cassidy FH, Ishioka KM, McMahon CJ (2010) MR imaging of scrotal tumors and pseudotumors. Radiographics 30:665–683. https://doi.org/10.1148/rg.303095049
16. Aganovic L, Cassidy F (2012) Imaging of the scrotum. Radiol Clin N Am 50:1145–1165. https://doi.org/10.1016/j.rcl.2012.08.003
17. Parenti GC, Feletti F, Carnevale A, Uccelli L, Giganti M (2018) Imaging of the scrotum: beyond sonography. Insights Imaging 9:137–148. https://doi.org/10.1007/s13244-017-0592-z
18. Tsili AC, Bertolotto M, Turgut AT, et al. (2018) MRI of the scrotum: recommendations of the ESUR Scrotal and Penile Imaging Working Group. Eur Radiol 28:31–43. https://doi.org/10.1007/s00330-017-4944-3
19. Tsili AC, Argyropoulou MI, Giannakis D, et al. (2012) Diffusion-weighted MR imaging of normal and abnormal scrotum: preliminary results. Asian J Androl 14:649–654. https://doi.org/10.1038/aja.2011.172
20. Algebally AM, Tantawy HI, Yousef RR, Szmigielski W, Darweesh A (2015) Advantage of adding diffusion weighted imaging to routine MRI examinations in the diagnostics of scrotal lesions. Pol J Radiol 80:442–449
21. Tsili AC, Ntorkou A, Astrakas L, et al. (2017) Diffusion-weighted magnetic resonance imaging in the characterization of testicular germ cell neoplasms: effect of ROI methods on apparent diffusion coefficient values and interobserver variability. Eur J Radiol 89:1–6. https://doi.org/10.1016/j.ejrad.2017.01.017
22. Tsili AC, Sylakos A, Ntorkou A, et al. (2015) Apparent diffusion coefficient values and dynamic contrast enhancement patterns in differentiating seminomas from nonseminomatous testicular neoplasms. Eur J Radiol 84:1219–1226. https://doi.org/10.1016/j.ejrad.2015.04.004
23. Tsili AC, Ntorkou A, Baltogiannis D, et al. (2015) The role of apparent diffusion coefficient values in detecting testicular intraepithelial neoplasia: preliminary results. Eur J Radiol 84:828–833. https://doi.org/10.1016/j.ejrad.2015.02.013
24. Watanabe Y, Dohke M, Ohkubo K, et al. (2000) Scrotal disorders: evaluation of testicular enhancement patterns at dynamic contrast-enhanced subtraction MR imaging. Radiology 217:219–227. https://doi.org/10.1148/radiology.217.1.r00oc41219
25. Tsili AC, Argyropoulou MI, Astrakas LG, et al. (2013) Dynamic contrast-enhanced subtraction MRI for characterizing intratesticular mass lesions. AJR Am J Roentgenol 200:578–585. https://doi.org/10.2214/AJR.12.9064
26. Manganaro L, Vinci V, Pozza C, et al. (2015) A prospective study on contrast-enhanced magnetic resonance imaging of testicular lesions: distinctive features of Leydig cell tumours. Eur Radiol 25:3586–3595. https://doi.org/10.1007/s00330-015-3766-4
27. Manganaro L, Saldari M, Pozza C, et al. (2018) Dynamic contrast-enhanced and diffusion-weighted MR imaging in the characterisation of small, non-palpable solid testicular tumours. Eur Radiol 28:554–564. https://doi.org/10.1007/s00330-017-5013-7
28. Sanharawi JE, Correas JM, Glas L, et al. (2016) Non-palpble incidentally found testicular tumors: differentiation between benign, malignant and burned-out tumors using dynamic contrast-enhanced MRI. Eur J Radiol 85:2072–2082. https://doi.org/10.1016/j.ejrad.2016.09.021
29. Tsili AC, Ntorkou A, Astrakas L, et al. (2017) Magnetic resonance diffusion tensor imaging of the testis: preliminary observations. Eur J Radiol 95:265–270. https://doi.org/10.1016/j.ejrad.2017.08.037

30. Tsili AC, Ntorkou A, Baltogiannis D, et al. (2016) Magnetization transfer imaging of normal and abnormal testis: preliminary results. Eur Radiol 26:613–621. https://doi.org/10.1007/s00330-015-3867-0
31. Firat AK, Uğraş M, Karakaş HM, et al. (2008) 1H magnetic resonance spectroscopy of the normal testis: preliminary findings. Magn Reson Imaging 26:215–220. https://doi.org/10.1016/j.mri.2007.06.008
32. Aaronson DS, Iman R, Walsh TJ, Kurhanewicz J, Turek PJ (2010) A novel application of 1H magnetic resonance spectroscopy: non-invasive identification of spermatogenesis in men with non-obstructive azoospermia. Hum Reprod 25:847–852. https://doi.org/10.1093/humrep/dep475
33. Tsili AC, Astrakas LG, Ntorkou A, et al. (2016) MR spectra of normal adult testes and variations with age: preliminary observations. Eur Radiol 26:2261–2267. https://doi.org/10.1007/s00330-015-4055-y
34. Baleato-González S, García-Figueiras R, Santiago-Pérez MI, Requejo-Isidro I, Vilanova JC (2015) Usefulness of 1H magnetic resonance spectroscopy in human testes: preliminary study. Clin Radiol 70:1026–1031. https://doi.org/10.1016/j.crad.2015.05.010
35. Tsili AC, Argyropoulou MI, Giannakis D, Sofikitis N, Tsampoulas K (2010) MRI in the characterization and local staging of testicular neoplasms. AJR Am J Roentgenol 194:682–689. https://doi.org/10.2214/AJR.09.3256
36. Tsili AC, Bertolotto M, Rocher L, et al. (2018) Sonographically indeterminate scrotal masses: how MRI helps in characterization. Diagn Interv Radiol 24:225–236. https://doi.org/10.5152/dir.2018.17400
37. Tsili AC, Tsampoulas C, Giannakopoulos X, et al. (2007) MRI in the histologic characterization of testicular neoplasms. AJR Am J Roentgenol 189:W331–W337. https://doi.org/10.2214/AJR.07.2267
38. Andipa E, Liberopoulos K, Asvestis C (2004) Magnetic resonance imaging and ultrasound evaluation of penile and testicular masses. World J Urol 22:382–391. https://doi.org/10.1007/s00345-004-0425-9
39. Thurnher S, Hricak H, Carroll PR, Pobiel RS, Filly RA (1988) Imaging the testis: comparison between MR imaging and US. Radiology 167:631–636. https://doi.org/10.1148/radiology.167.3.3283834
40. Johnson JO, Mattrey RF, Phillipson J (1990) Differentiation of seminomatous from nonseminomatous testicular tumors with MR imaging. AJR Am J Roentgenol 154:539–543. https://doi.org/10.2214/ajr.154.3.2106218
41. Schultz-Lampel D, Bogaert G, Thüroff JW, Schlegel E, Cramer B (1991) MRI for evaluation of scrotal pathology. Urol Res 19:289–292. https://doi.org/10.1007/BF00299060
42. Rocher L, Ramchandani P, Belfield J, et al. (2016) Incidentally detected non-palpable testicular tumours in adults at scrotal ultrasound: impact of radiological findings on management radiologic review and recommendations of the ESUR scrotal imaging subcommittee. Eur Radiol 26:2268–2278. https://doi.org/10.1007/s00330-015-4059-7
43. Tsitouridis I, Maskalidis C, Panagiotidou D, Kariki EP (2014) Eleven patients with testicular leydig cell tumors: clinical, imaging, and pathologic correlation. J Ultrasound Med 33:1855–1864. https://doi.org/10.7863/ultra.33.10.1855
44. Syer TJ, Godley KC, Cameron D, Malcolm PN (2018) The diagnostic accuracy of high b-value diffusion- and T2-weighted imaging for the detection of prostate cancer: a meta-analysis. Abdom Radiol 43:1787–1797. https://doi.org/10.1007/s00261-017-1400-4
45. Wibmer AG, Sala E, Hricak H, Vargas HA (2016) The expanding landscape of diffusion-weighted MRI in prostate cancer. Abdom Radiol 41(5):854–861. https://doi.org/10.1007/s00261-016-0646-6
46. Wang WJ, Pui MH, Guo Y, et al. (2014) 3T magnetic resonance diffusion tensor imaging in chronic kidney disease. Abdom Imaging 39:770–775. https://doi.org/10.1007/s00261-014-0116-y
47. Razek AAKA, Al-Adlany MAAA, Alhadidy AM, Atwa MA, Abdou NEA (2017) Diffusion tensor imaging of the renal cortex in diabetic patients: correlation with urinary and serum biomarkers. Abdom Radiol (NY) 42:1493–1500. https://doi.org/10.1007/s00261-016-1021-3
48. Argyropoulou MI, Kiortsis DN, Metafratzi Z, Efremidis SC (2000) Magnetization transfer imaging of the normal adenohypophysis: the effect of sex and age. Neuroradiology 43:305–308. https://doi.org/10.1007/s0023400004
49. Vilanova JC, Barceló J (2007) Prostate cancer detection: magnetic resonance (MR) spectroscopic imaging. Abdom Imaging 32:253–261. https://doi.org/10.1007/s00261-007-9191-7
50. Casciani E, Polettini E, Bertini L, et al. (2007) Contribution of the MR spectroscopic imaging in the diagnosis of prostate cancer in the peripheral zone. Abdom Imaging 32:796–802. https://doi.org/10.1007/s00261-007-9181-9